Surface Science 90 (1979) 240–255

ION-INDUCED ELECTRON EMISSION FROM CLEAN METALS *

R.A. BARAGIOLA, E.V. ALONSO, J. FERRON and A. OLIVA-FLORIO
Centro Atómico Bariloche, Comisión Nacional de Energía Atómica, Instituto Balseiro, Universidad Nacional de Cuyo, 8400 S.C. de Bariloche, R.N., Argentina

Received 23 October 1978; manuscript received in final form 27 December 1978

We report recent experimental work on electron emission from clean polycrystalline metal surfaces under ion bombardment. We critically discuss existing theories and point out the presently unsolved problems.

1. Introduction

Electron emission (EE) is one of the most conspicuous effects of the interaction of atomic particles with solids. Research in this field started 80 years ago and developed not only from basic physical interest but from the appreciation that this research was important in the understanding of electrical discharges, in the development of particle multipliers for mass spectrometry and in experimental atomic collisions physics. Ion induced EE is being applied nowadays also in studies of the electronic properties of solid surfaces and in fast-timing detectors for swift heavy ions, and its occurrence is important in nuclear fusion devices.

The work intended for applications has generally been performed with ill-defined surfaces, while most of the basic work predates ultrahigh vacuum and modern surface cleaning techniques. In particular, the appreciation that most surfaces cannot be cleaned by heating alone in vacuo is absent in the majority of the research reported in the last major reviews of the field (1–6); this is very unfortunate since EE depends dramatically on the state of the target surface.

Ion induced EE can proceed by two distinct processes. In potential EE (PEE), which is analogous to Penning ionization in gas-phase atomic collisions, the potential energy released upon neutralization of the projectile ion can provide the energy required to free electrons from the solid. This process can occur if the ground-state neutralization energy of the ion, E_i, exceeds twice the workfunction of the solid,

* Work partially supported by the International Atomic Energy Agency under Contract No. 1928/RB and by the Multinational Program in Physics of the Organization of American States.

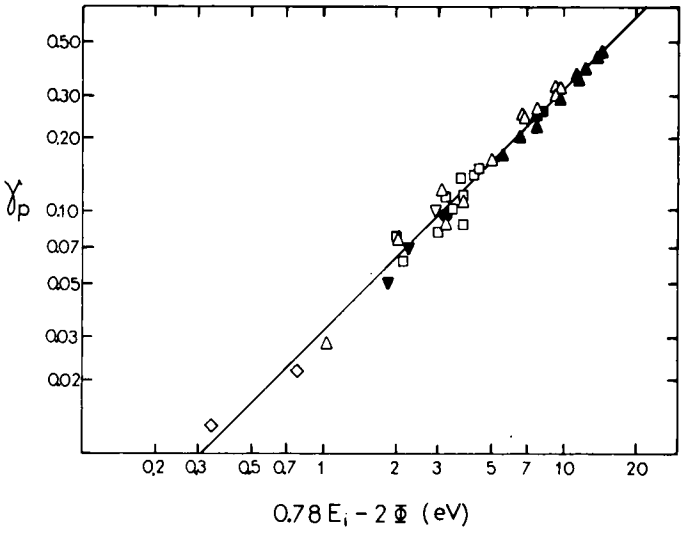

Fig. 1. PEE yields γ_p versus $0.78E_i - 2\phi$; (▲, △) Arifov [6] for Ne^+ and Ar^+ ions respectively; (●, ▽, ▼, ◇, ■) Hagstrum [7] for He^+, Ne^+, Ar^+, Kr^+ and Xe^+ ions respectively; (□) Oechsner [9] for Ar^+ ions. The line is a least-square fit.

ϕ, and being exothermic, it has no kinetic threshold. Different mechanisms of PEE have been discussed by Hagstrum [7]; it is found that present semi-empirical theories [7,8] work satisfactorily at small projectile velocities. Fig. 1 shows a compilation of PEE yields γ_p (number of electrons emitted per incident ion) obtained for noble gas ions on polycrystalline metal surfaces [6,7,9]. The yields are seen to fall in a narrow band around $\gamma_p = 0.032(0.78E_i - 2\phi)$ (least square fit), the spread being smaller than that obtained using Kishinevskii's formula [8], $\gamma_p = 0.2(0.8E_i - 2\phi)/E_F$, where E_F is the Fermi energy.

For ion velocities larger than about 10^7 cm/s, kinetic EE (KEE) becomes relatively more important than PEE. In this process the energy necessary to eject electrons into vacuum is provided by the kinetic energy of the projectile.

In this work we will review our recent work on ion induced EE from clean polycrystalline surfaces in the KEE energy range and we will discuss existing theories in the light of the experimental evidence.

2. Experimental approach

Fig. 2 shows the experimental apparatus [10]. The monoenergetic ion beam is produced by a 60 kV accelerator and is mass analyzed with a double-focusing magnet with a mass resolution of ca. 100. In the determination of the beam energy due

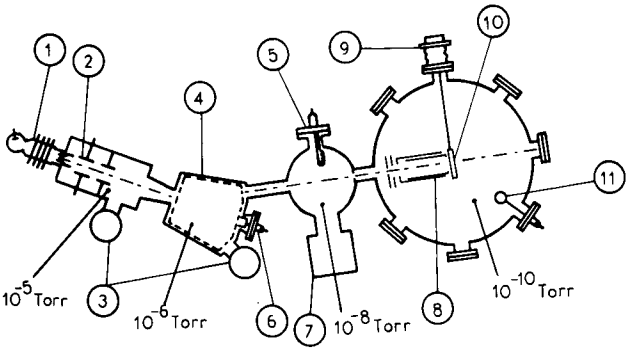

Fig. 2. Experimental apparatus: 1 rf ion source, 2 focusing lens, 3 diffusion pumps, 4 mass-sorting magnet, 5 titanium sublimator, 6 Faraday cup, 7 ion pump, 8 collector assembly, 9 manipulator, 10 target, and 11 quartz-crystal resonator.

due account is taken of the excess energy due to the plasma potential in the ion source; the energy of the ions is thus known to within (±0.1% + 30 eV). In order to minimize the flow of gases from the accelerator to the target chamber, several stages of differential pumping are used. The pressure in the UHV target chamber is kept in the 10^{-10} Torr range. Clean targets are produced by in situ evaporation in UHV of high-purity (better than 99.9%) materials or by sputtering with argon ions. In order to minimize the contamination of the target by trapped ions when bombarding with reactive ions, total doses were kept small ($<10^{13}$ ions/cm^2). The target-collector system is described in detail elsewhere [10]; considerable care was taken in its design to avoid spurious results by preventing scattered beam particles from hitting the collector or the suppressor electrode. Systematic errors due to the presence of neutrals in the beam, sputtered and backscattered ions, together with statistical uncertainties, amounted to ±4%.

3. Results

3.1. Influence of target condition

The equivalence of using clean surfaces produced by evaporation or by sputtering has been checked for different targets. Fig. 3 shows the variation of the yield with ion dose when a pure Al sample with an air-formed oxide is cleaned with 30 keV Ar^+ ions; the yield obtained for high doses is seen to correspond very well to that obtained from a freshly evaporated film.

A general picture of the spread in the data taken by different authors [11–24] using different experimental techniques is shown in fig. 4 for Ar on Al. Good agreement exists only between experiments performed under conditions such that the rate of removal of adsorbed atoms by sputtering greatly exceeded the rate of

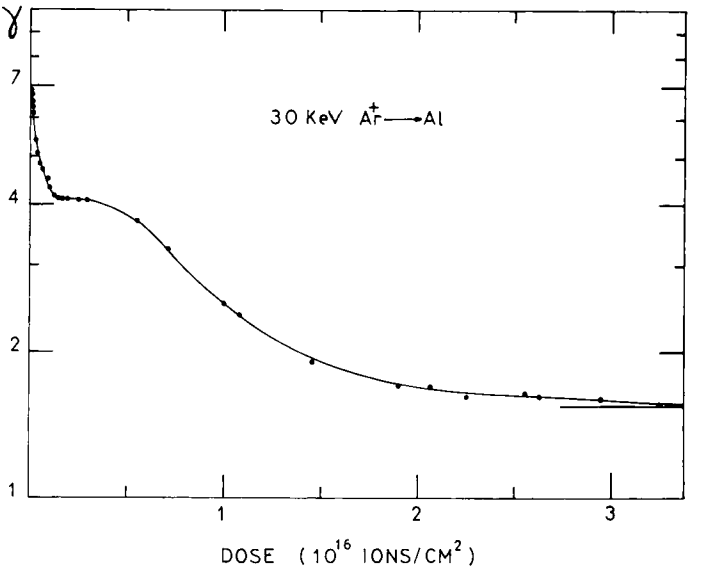

Fig. 3. Electron yields γ versus ion dose for 30 keV Ar^+ on an Al sample initially covered with an air-formed oxide. The horizontal line at high doses represent the yield obtained from an Al film immediately after in-situ deposition in UHV.

adsorption. Some data lie beyond the limits that could be expected from the results of fig. 3 indicating that effects other than contamination were present, the most common drawbacks of early work were that the projectile beam used was not mass analyzed, that it contained a sizable fraction of neutral atoms and that it could hit the suppressor electrode.

3.2. Yields for atomic ions

Figs. 5 and 6 show results for hydrogen and helium ions respectively on Li, Al, Cu and Ag. No evidence for isotope effects was observed within errors in the yields for equal velocity H^+ and D^+ in our velocity range. Isotope effects are to be expected at very low velocities where backscattering, energy degradation, energy and angular straggling of the projectiles over the effective electron escape depths are important, since these effects are known to show a mass dependence. In the case of He^+ projectiles, PEE contributes substantially to the yields in our energy range due to the large ionization energy of helium (see fig. 1); this is probably also true for H^+ on lithium due to the very low ionization potential of this metal. For velocities larger than about 5×10^7 cm/s the yields for He^+ are found to be roughly twice the yields for H^+ with the same velocity. At velocities much higher than those used in this work we should expect on general grounds that the ratios of the yields for He^+ and H^+ should tend to $Z^2(\mathrm{He})/Z^2(\mathrm{H}) = 4$.

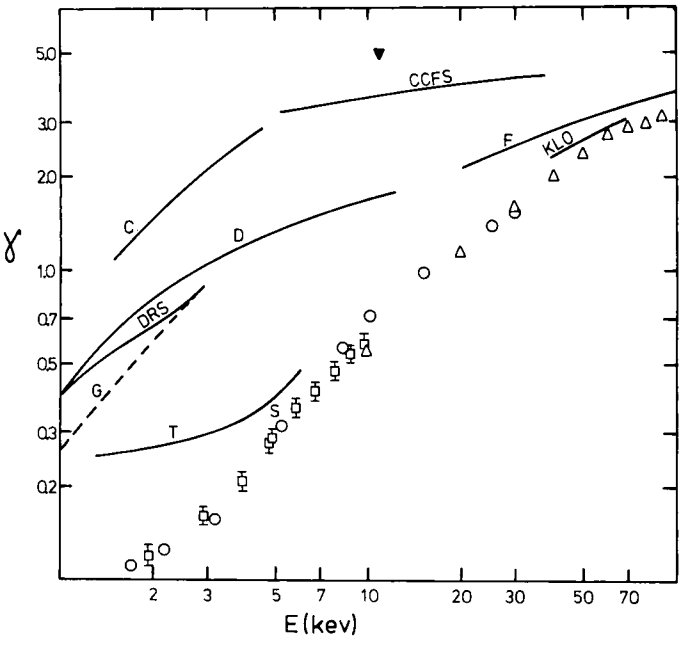

Fig. 4. Electron yields for Ar on Al: (G) [11] measured in a discharge; (T) [12]; (CCFS) [14]; (F) [15]; (S) [16]; (□) [17]; (D) [21] for Ar^0; (▾) [19] for Ar^0; (C) [20] for Ar^0; (DRS) [18] for Ar^0; (KLO) [22,23]; (△) [24] data for 60° incidence normalized to 0° by dividing by 2 = $\cos^{-1}$ (60°); (○) this work, errors ±4%. Not shown are the data of ref. [13], γ = 12.9 at 5 keV.

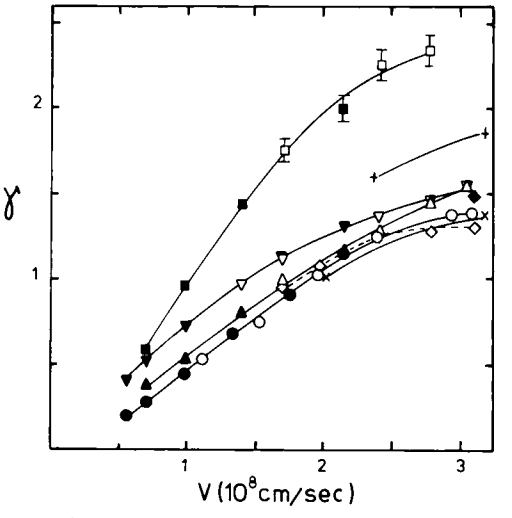

Fig. 5. Electron yields for H^+ (open symbols) and D^+ (filled symbols): (▽, ○, △, □) Li, Al, Cu and Ag, respectively [10]; (◆) Cu from ref. [25]; (◇) Al from ref. [24], data for 60° incidence normalized to 0° by dividing by 2; (×, +) Cu and Ag respectively [27].

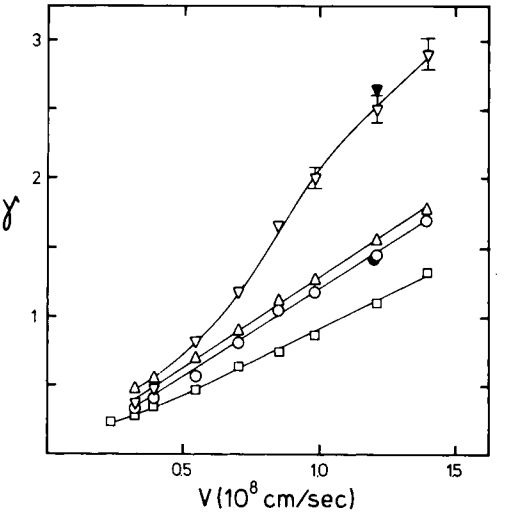

Fig. 6. Electron yields for He^+: (△, □, ○, ▽) Li, Al, Cu and Ag, respectively, from ref. [10]; (●) Cu and (▼) Ag from ref. [26].

In figs. 5 and 6 we have plotted also the results of other workers who took care to obtain reasonably clean surfaces. Good agreement is observed with data of Wurtz and Tapp [25] for D^+ on Cu and of Evdokimov et al. [26] for He^+ on Cu and Ag. The results of Large and Whitlock [27] for H^+ are somewhat lower than ours; these workers attempted to clean their very thin (50 μm) targets by heating, a procedure which not only would cause the surface segregation of bulk impurities but could also lead to the growth of grains with preferred orientation (the foils were probably rolled) thus causing some channeling of the H^+ and consequently lower yields [28–30].

Figs. 7 and 8 show yields for Ar and Kr ions on different solids. Good agreement is again obtained with data of Evdokimov et al. [26,31]; on the other hand the data of Magnuson and Carlston [17] which was shown to agree with ours for Ar^+ on Al (fig. 4) does so also for Kr^+ on Cu but is quite lower than ours for Ar^+ on Cu. Heavy ions are seen to give yields substantially higher than H^+ and He^+ when compared at the same velocity; yields grow initially linearly with energy and then with velocity.

Fig. 9 shows the dependence of the yields at 30 keV on Z_1, the atomic number of the projectile for several targets. Some regularities are apparent except for Al in which $\gamma(H) > \gamma(He)$. The fall for Ar in the heavy targets is probably due to a large energy loss of these ions within the mean electron escape depth in those targets. Fig. 10 shows the dependence of the yields at 30 keV on Z_2, the atomic number of the target, for different projectiles. Also plotted are the maximum values of the secondary EE yields under electron bombardment [32]. Similarities are again found

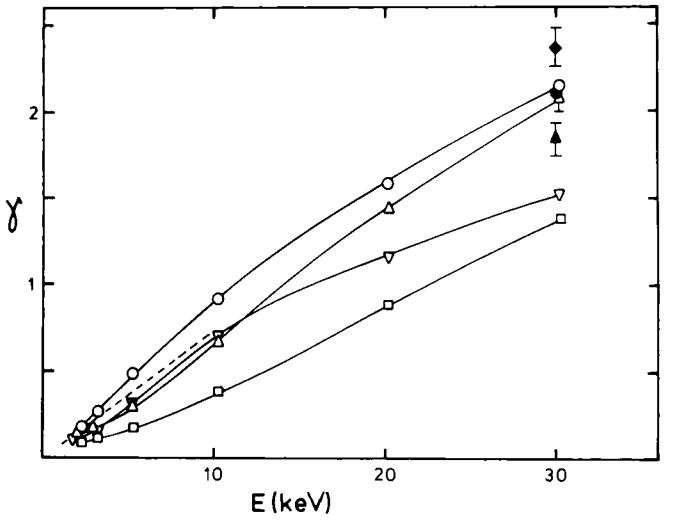

Fig. 7. Electron yields for Ar^+: (▽) Al, (○) Cu, (△) Ag and (□) Au, this work; (●) Cu from ref. [31]; (◆) Cu, (▲) Ag from ref. [26]; (– – –) Cu from ref. [17].

albeit with some irregularities. In particular, the yields for electron impact grow on the average faster with Z_2 than those for ions; this is probably due to the influence of backscattered electrons in the yields.

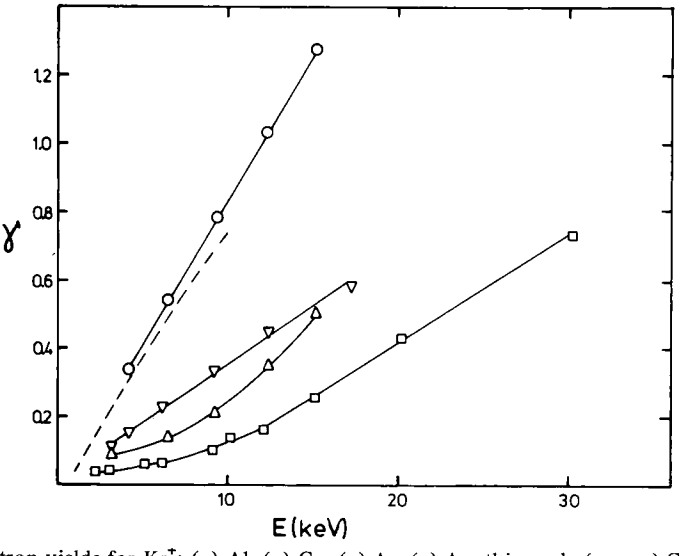

Fig. 8. Electron yields for Kr^+: (▽) Al, (○) Cu, (△) Ag, (□) Au, this work; (– – –) Cu from ref. [17].

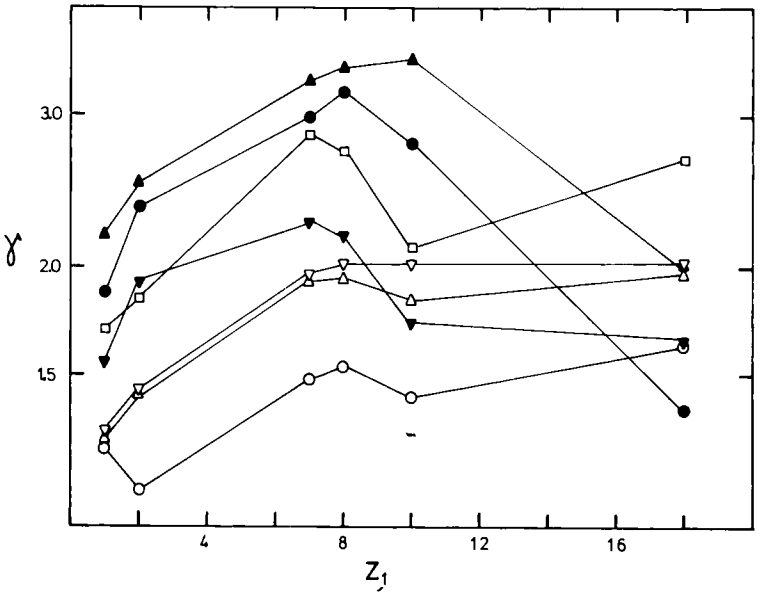

Fig. 9. Z_1 dependence of the EE yields for (□) C, (○) Al, (△) Cr, (▽) Cu, (▼) Mo, (▲) Ag, and (●) Au, at 30 keV.

3.3. Yields for molecular ions

In the few experiments made in the past using light molecular ions as projectiles it was generally found that the yields for these ions were slightly smaller than the

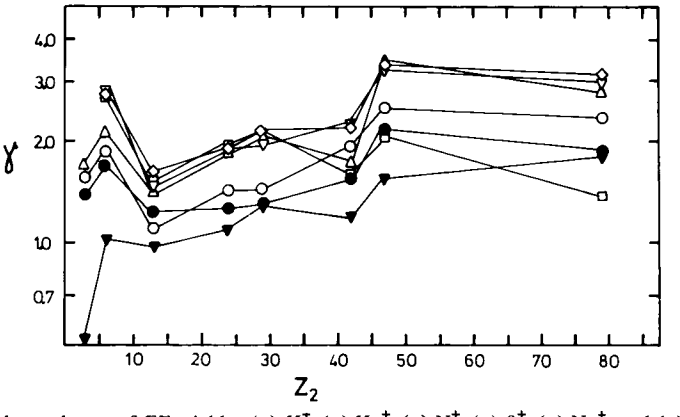

Fig. 10. Z_2 dependence of EE yields: (●) H^+, (○) He^+, (▽) N^+, (◇) 0^+, (△) Ne^+, and (□) Ar^+ at 30 keV. ▼ maximum values of the secondary EE yields under electron bombardment [32].

sum of the yields for each component of the molecule at the same velocity v; for diatomic ions: $\gamma(X_2^+, v)/2 < \gamma(X^+, v)$.

This effect was first noticed by Hill et al. [33] and discussed recently by Baragiola et al. [34]. Molecular effects can be significant for very light ions and values of the ratio $R = 2\gamma(X^+, v)/\gamma(X_2^+, v)$ up to ~1.2 have been measured for hydrogen ions on Al at velocities where PEE is thought to be unlikely. With the exception of oxygen ions on Al for which R is again about 1.2 at high energies, data for nitrogen and oxygen ions show a small molecular effect. A complication in these experiments exists, however, since the N^+ and O^+ ion beams contained an unknown fraction of N_2^{2+} and O_2^{2+} ions, respectively, which could not be separated.

Values of R much larger than 1 occur in the low velocity regime where PEE predominates; this reflects the very small PEE yields for molecular ions as compared with atomic ions [35]. Molecular effects in our energy range have also been observed in ionization in gas-phase atomic collisions [36] and in the electronic energy loss of ions in solids [37,38].

At velocities larger than those used in this work, electron loss from the projectile will give an additional contribution to the KEE yield. This effect will act in an opposite way as that discussed above since it will contribute for example to $\gamma(H_2^+)$ but not to $\gamma(H^+)$.

4. Theory

Different theories of ion-EE have been reviewed by Arifov [6] and by Parilis [39]. Of those, the ones that have been more succesful when compared to experiment are those published by Sternglass [40], Ghosh and Khare [41], Parilis and Kishinevskii [42,43] and Harrison et al. [44]. We will briefly describe these theories and evaluate them on the light of physical principles and observations.

4.1. Theory of Sternglass

This author considers that EE results from the excitation of target electrons in hard collisions with the projectile (δ-ray formation) and so writes for the number of electrons excited at depth x by a fast charge of velocity v_i:

$$n(v_i, x) = (1/\bar{E}_0) \times \tfrac{1}{2} S_i \, k(v_i, x), \tag{1}$$

where $\bar{E}_0$ is the mean energy loss per excited electron formed in the *primary* interaction, S_i the total electronic energy loss per unit path length and $k(v_i, x)$ a factor representing the electron excitation produced by the δ-rays and which takes into account the anisotropy of the electron cascade. The factor 1/2 in the energy loss enters because Sternglass assumes [redacted] equipartition of energy loss in hard and soft collisions (Bohr's rule [45]). The theory neglects [redacted] EE from the decay of plasmons. Further-

more, the equipartition rule is not valid in the form commonly used, as shown by Lindhard and Winter [46] and, as a consequence, eq. (1) underestimates the production of excited electrons even more.

The yield is finally given by:

$$\gamma = \int_0^\infty \frac{S_i}{2\bar{E}_0} Pk(v_i, x) \exp\left(-\frac{x}{L}\right) dx , \tag{2}$$

where L is the mean electron attenuation length, and P the surface transmission probability. Sternglass estimates P to be about 0.5 and in so doing he neglects the inner potential seen by the electron in the bulk on the basis that these excited electrons are very energetic. This argument is incorrect since the average energy of the emitted electrons lies only about 10 eV with respect to the Fermi level. Sternglass uses for E_0, the mean energy required to form an electron–hole pair J (of the order of 20–30 eV). However by his definition $\bar{E}_0$ does not take into account secondary ionization whereas J does. The theory was shown to be in good agreement with the experimental data of Hill et al. [33] and Aarset et al. [47] for 0.1–2 MeV H^+ on different metals. This agreement must be considered fortuitous according to the points made above, to the fact that the Bethe theory for S_i is used (at low v_i) outside its range of validity and to the fact that the mentioned experiments were conducted with contaminated targets which give yields much higher than clean targets [25,27,30] in this energy range.

4.2. Theory of Ghosh and Khare

The treatment of these workers is based on the assumption that $n(v_i, x)$ is proportional to an ionization cross section σ such as those derived for gas-phase collisions. This gives very little weight to the excitation of inner-shell electrons and it effectively neglects the cascade (secondary ionization) and Auger processes. Since σ and S_i have a similar energy dependence in the range 0.1–2 MeV, these authors could fit the data of Hill et al. [33] and Aarset et al. [47] on contaminated surfaces; in doing so, however, they arrived at the unreasonable [48] value of 120 Å for the mean electron escape depth in Al. The surface transmission probability P was also taken in this work to be equal to 0.5.

4.3. Theory of Parilis and Kishinevskii

These workers consider that the excitation of nearly free valence band electrons in metals by low energy ions is very unlikely and assume that EE is caused primarily by the Auger decay of inner-shell vacancies in the target atoms produced in collisions with the projectile. To evaluate the cross section for inner-shell hole production they calculate, using a modification to a theory by Firsov [49], the energy lost by the projectile to excitations above a threshold $\delta - \phi$, $E(\delta - \phi)$, and divide

it by a mean energy J spent in these excitations. Here δ is the binding energy of the core electron measured from the vacuum level, and J is given by Parilis and Kishinevskii (PK) the value ~30 eV.

Fundamental faults can be seen at this point. First, the Firsov theory calculates the energy loss to the electronic system in a collision in which the valence electrons are also involved; on the other hand, PK use this energy loss in which all electrons are involved but apply it to the excitation of core electrons only. Second, the value of 30 eV for J refers to total ionization, again including the valence band, and takes into account as well secondary ionization by the excited electrons. This value should not be used for the innershells, specially since $J < \delta - \phi$ in most cases. All this will result in a considerable overestimate of the inner-shell ionization cross section. To calculate the electron yield γ, PK use the formula:

$$\gamma = W(\delta) N \int_0^\infty \frac{E(\delta - \phi)}{J} \exp\left(-\frac{x}{L}\right) \mathrm{d}x \,, \tag{3}$$

where E is a function of the velocity of the projectile v which in turn is a function of the depth of penetration x, N is the target number density, L the mean electron attenuation length and W the probability that the Auger process results in electron ejection in the absence of attenuation. W is taken by PK from data on PEE by Auger neutralization. It should be noted that the excitation of projectile electrons has not been considered in this model.

Baklitsky et al. [50] further developed the theory modifying the Firsov model which is based on a Thomas–Fermi description of the colliding system, using free-atom Hartree–Fock–Slater wavefunctions and so predicted an oscillatory behaviour of the yields as a function of Z_1. The neglect of the excitation of projectile electrons was kept. The sophistication of using atomic HFS orbitals has also been carried out before in calculations [51] of stopping powers at low velocities in modified Firsov models. This is not justified since a description of the wavefunctions of the quasi-molecule formed in the collision using atomic orbitals is incorrect at these low velocities and since in any case the use of outer-shell wavefunctions of free atoms is meaningless in the case of projectiles colliding with atoms in condensed matter.

PK obtain a final threshold velocity for EE of $(6–7) \times 10^6$ cm/s, which is higher than those found in most experimental observations. The theory correctly predicts the yields to grow linearly with energy near the threshold and then to grow linearly with velocity. This is however not a property of the PK model but is intrinsic to the Firsov theory when energy transfers above a minimum value are considered. PK show in their paper [42] theoretical curves which were made to fit very well with experimental data for Ar^+ and Kr^+ ions on Mo and Ar^+ on W by suitable choices of J. However, the calculations are based on values of δ of 16 and 19 eV for Mo and W respectively derived from early electron energy loss measurements by Harrower who interpreted some peaks in his spectra to arise from core-level excitations [52].

These peaks were later correctly attributed to the excitation of plasmons [53] so that the proper values of δ are instead about 40 eV. With these values it is now impossible to fit the data well since particularly the threshold velocity becomes too large.

Recent work on the emission of Auger electrons in ion–solid interactions [54,55] casts further doubt on the importance of the Auger mechanism in low energy KEE. In these works the Auger yields are found to vary very strongly with Z_1 and Z_2 and also with impact energy. This is very unlike the results which are found for the total electron yields.

4.4. Theory of Harrison, Carlston and Magnuson

These workers consider the case of impact energies below 10 keV for heavy ions. They assume that all emitted electrons come from the projectile, in contradistinction with PK, and as a result of collisions involving only surface and near-surface atoms. The inelastic energy loss is derived from the Firsov theory using a very hard interatomic potential and a "maximum" impact parameter. The number of excited electrons is obtained from the statistical model of Russek [56]. The theory has been applied to measurements in single crystal and its evident limitations are not apparent in the comparison with experiment due to the use of several fitting parameters and the intrinsic uncertainties in the models of Firsov and Russek and in the choice of ionization potentials for ions in solids which are required in the latter model.

4.5. Excitation of valence electrons

It was shown above that the neglect of the excitation of these target electrons lead to results in disagreement with experiment. Let us consider first the excitation of free electrons by light ions [10]; in this case the maximum energy that can be transferred in a direct binary interaction is:

$$T_m = 2\, mv(v + v_F), \tag{4}$$

where m is the electron mass, v the velocity of the ion and v_F the velocity of the electrons at the Fermi surface. In this model, a threshold velocity exists when $T_m = \phi$, and is given by:

$$v_{th} = \tfrac{1}{2} v_F \left[(1 + \phi/E_F)^{1/2} - 1\right], \tag{5}$$

where $E_F = \frac{1}{2} m v_F^2$ is the Fermi energy.

The fact that valence electrons are not really free will cause the maximum energy transfer to be larger than that given in (4) and correspondingly v_{th} will be smaller than in (5). Nevertheless it has been shown that the extrapolation of the yields for H^+ to very low velocities is not inconsistent with eq. (4). Measurements below 100 eV for neutral ground state H for which the PEE yields are zero are

needed to test conclusively the validity of (5).

The inefficient energy transfer mechanism described for light ions is due to the effect of the large difference in mass between the ion and the electron in the direct screened Coulomb interaction. For the case of heavy projectiles which carry electrons into the collisions, the situation is different since then electron–electron interactions give rise to more efficient excitation as the electron clouds are compressed during the collision. This excitation mechanism, often referred to as electron promotion or Pauli excitation is well known to occur in inner-shell excitation processes [57]. Then, for heavy ions, the maximum energy transfer and the threshold velocities for EE should be higher and lower than those given in eqs. (4) and (5) respectively. It is worth noting here that the picture of a nearly-free valence electron gas loses its meaning in the case of heavy ions moving slowly in solids since the localized dynamic perturbation which is set in the system is very strong. The situation will resemble more the case of atomic collisions in gases except for transitions which occur at large internuclear distances and for the fact that final states are different, i.e., the minimum energy transfer required for EE will be ϕ.

4.5. Final remarks

In analogy with semiempirical theories of secondary EE under electron bombardment [58] and partly in analogy with Sternglass and PK, we can write, for the electron yield at velocities much larger than v_{th}:

$$\gamma = P \int_{\infty}^{0} n(v, x) f(x)\, dx = \frac{P}{2J} \int_{0}^{\infty} S_i(v, x) \exp\left(-\frac{x}{L}\right) dx , \tag{6}$$

where $f(x) = \frac{1}{2} \exp(-x/L)$ is the attenuation function, P the surface escape probability, S_i the total inelastic stopping power and J the average energy required to form an electron–hole pair with the electron energy above the vacuum level. Eq. (6) can be simplified further by noting that at velocities where it is valid, v does not vary much within distances of order L; therefore one can take S_i out of the integral and obtain:

$$\gamma(v_i) = PLS_i(v_i)/2J, \tag{7}$$

with the important consequence that the yields should be proportional to the electronic stopping power. As a matter of practical importance, we have found in all the targets for which both γ and S_i have been measured and for v larger than 7×10^7 cm/s the following formula to hold within ±40%

$$\gamma(v) = 0.1\, S_i(v)\ (\text{Å/eV}). \tag{8}$$

It should be noted that so far we have neglected EE by recoiling target atoms, an effect which should be important when the mass of the projectile is larger than that of the target atom. In this case, S_i should be replaced by F_i, the total inelastic

energy loss per unit depth interval, and since, in general, the average recoil velocity will be small we must use:

$$\gamma(v) = \frac{P}{2J'} \int_0^\infty F_i(v, x) \exp\left(-\frac{x}{L}\right) dx \,, \tag{9}$$

The dependence of the yields on Z_1 and Z_2 is, as we have seen, very complicated. As electrons from the projectile and the target can be excited, J' should be a function of both Z_1 and Z_2, and so should be F_i. The quantities P and L which so far have been assumed to be characteristic of the target could also depend on Z_1 for slow heavy projectiles. This is because these atoms move much slower than the average electron in the cascade and so could perturb both the transport and escape of the excited electrons.

5. Unsolved problems

This concluding section has as goals to draw attention to some major unsolved problems and to summarize the information surveyed.

The first problem encountered in trying to analyze yields at low velocities was how to separate PEE from KEE. The available knowledge does not allow us to estimate the magnitude of PEE beyond the threshold for KEE; in particular, the velocity dependence of PEE remains unknown.

The inelastic energy transfer at low velocities is not well known specially regarding the impact parameter dependence and the Z_1, Z_2 oscillations.

The yields can be described by a semiempirical formula which in principle takes into account single particle and collective excitations in the Fermi sea, excitation of bound states and Auger decay of inner-shell holes and two-electron outer-shell excitations. The value of the average energy to form an electron–hole pair near the kinetic threshold and at high velocities can, on the other hand, be estimated only very crudely.

The transport and escape of excited electrons in solids with due account of band structure effects is still unsolved, even in more developed fields of photo- and secondary-electron emission. In the case of ion induced EE a further complication arises at low impact velocities due to the perturbation set by the projectile on the excited electrons.

Finally, the reason for the extreme sensitivity of EE to adsorbed gas remains obscure although the effect has been known for several decades.

In conclusion, we feel that much progress could be made from studies of inelastic energy loss in low-velocity heavy-ion collisions, in angle-resolved electron energy distributions, in coincidence experiments between sputtered or backscattered ions and electrons and in the variation of EE yields with adsorption of different gases, preferently in single crystals and using complementary techniques

to measure simultaneously the changes in work function, in the density of states and in the geometrical disposition of the adsorbates.

Acknowledgements

We would like to thank O. Auciello, G. Lantschner and H. Raiti for their help in the setup of the experiments. We are also indebted to N. Arista and W. Brandt for useful discussions.

References

[1] M. Kaminski, Atomic and Ionic Impact Phenomena on Metal Surfaces (Springer, Berlin, 1965).
[2] D.B. Medved and I.S. Strausser, Advan. Electron. Electron Phys. 21 (1965) 101.
[3] I.A. Abroyan, M.A. Eremeev and N.N. Petrov, Soviet Phys.-Usp. 10 (1967) 332.
[4] K.H. Krebs, Fortschr. Physik 16 (1968) 419.
[5] G. Carter and J.S. Colligon, Ion Bombardment of Solids (Heinemann, London, 1968).
[6] U.A. Arifov, Interaction of Atomic Particles with a Solid Surface (Consultants Bureau, New York, 1969).
[7] H.D. Hagstrum, in: Inelastic Ion–Surface Collisions, Eds. N.H. Tolk et al. (Academic Press, New York, 1977) p. 1.
[8] L.M. Kishinevskii, Radiation Effects 19 (1973) 23.
[9] H. Oechsner, Phys. Rev. B17 (1978) 1052.
[10] R.A. Baragiola, E.V. Alonso and A. Oliva-Florio, Phys. Rev. B19 (1979) 121.
[11] A. Guntherschulze, W. Bar and A. Winter, Z. Physik 111 (1938) 208.
[12] G. Timoshenko, J. Appl. Phys. 12 (1941) 69.
[13] G. Slodzian, Compt. Rend. (Paris) 246 (1958) 3631.
[14] P. Cousinié, N. Colombié, C. Fert and R. Simon, Compt. Rend. (Paris) 249 (1959) 387.
[15] C. Fert, N. Colombié, B. Fagot and P. Van Chuong, Colloq. Intern. CNRS (Paris) 113 (1962) 67.
[16] H. Schirrwitz, Beiträge Plasmaphysik 2 (1962) 188.
[17] G.D. Magnuson and C.E. Carlston, Phys. Rev. 129 (1963) 2403.
[18] F.M. Devienne, J.C. Roustan and J. Souquet, Compt. Rend. (Paris) 260 (1965) 4701.
[19] P. Schackert, Z. Physik 197 (1966) 32.
[20] L.E. Collins and P.T. Stroud, Brit. J. Appl. Phys. 18 (1967) 1121.
[21] F.M. Devienne, J. Physique 28 (1967) 602.
[22] V.I. Krotov, S.Ya. Lebedev and N.M. Omel'yanovskaya, Radio Eng. Electron. Phys. 14 (1969) 1938.
[23] S.Ya. Lebedev, N.M. Omel'yanovskaya and V.I. Krotov, Soviet Phys.-Solid State 11 (1969) 1294.
[24] N. Benazeth, private communication.
[25] J.L. Wurtz and C.M. Tapp, J. Appl. Phys. 43 (1972) 3318.
[26] I.N. Evdokimov, E.S. Mashkova, V.A. Molchanov and D.D. Odintsov, Phys. Status Solidi 19 (1967) 407.
[27] L.N. Large and W.S. Whitlock, Proc. Phys. Soc. (London) 79 (1962) 148.
[28] M. Kaminsky and G. Goodwing, Rept, ANL-7081 (1965).
[29] M. Kaminsky, Rept. ANL-7108 (1966).

[30] R.I. Ewing, Phys. Rev. 166 (1968) 324.
[31] I.N. Evdokimov, V.A. Molchanov, D.D. Odintsov and V.M. Tshitsherov, Soviet Phys.-Solid State 8 (1967) 2348.
[32] D.J. Gibbons, in: Handbook of Vacuum Physics, Vol. 2, Ed. A.H. Beck (Pergamon, Oxford, 1960) pt. 3.
[33] A.G. Hill, W.W. Buechner, J.S. Clark and J.B. Fisk, Phys. Rev. 55 (1939) 463.
[34] R.A. Baragiola, E.V. Alonso, O. Auciello, J. Ferrón, G. Lantschner and A. Oliva-Florio, Phys. Letters 67a (1978) 211.
[35] F.M. Propst and E. Luescher, Phys. Rev. 132 (1963) 1037.
[36] V.V. Afrosimov, R.N. Il'in and N.V. Fedorenko, Soviet Phys.-Tech. Phys. 3 (1958) 2080; Soviet Phys.-JETP 34 (1958) 968.
[37] V.V. Makarov and N.N. Petrov, Soviet Phys.-Solid State 8 (1966) 3723.
[38] J.C. Eckhardt, G. Lantschner, N.R. Arista and R.A. Baragiola, J. Phys. C. (Solid State Phys.) 11 (1978) 1851.
[39] E.S. Parilis, Radio Eng. Electron. 7 (1962) 1839.
[40] E.J. Sternglass, Phys. Rev. 108 (1957) 1.
[41] S.N. Ghosh and S.P. Khare, Phys. Rev. 125 (1962) 1254.
[42] E.S. Parilis and L.M. Kishinevskii, Soviet Phys.-Solid State 3 (1960) 885.
[43] L.M. Kishinevskii and E.S. Parilis, Bull. Acad. Sci. USSR, Phys. Ser. 26 (1962) 1432.
[44] D.E. Harrison, C.E. Carlston and G.D. Magnuson, Phys. Rev. 139 (1965) A737.
[45] N. Bohr, Mat. Fys. Medd. Dan. Vid. Selsk. 18 (1948) 8.
[46] J. Lindhard and A. Winther, Mat. Fys. Medd. Dan. Vid. Selsk. 34 (1964) 4.
[47] B. Aarset, R.N. Cloud and J.G. Trump, J. Appl. Phys. 25 (1954) 1365.
[48] L.M. Bronstein and B.S. Fraiman, Soviet Phys.-Solid State 3 (1961) 1188;
J.C. Noiray, R. Bindi, H. Lanteri, F. Martin and J. Borgnino, Thin Solid Films 23 (1974) 63.
[49] O.B. Firsov, Soviet Phys.-JETP 9 (1959) 1076.
[50] B.E. Baklitsky and E.S. Parilis, Radiation Effects 12 (1972) 137;
B.E. Baklitsky, E.S. Parilis and V.K. Verleger, Radiation Effects 19 (1973) 155.
[51] K.B. Winterborn, Can. J. Phys. 46 (1968) 2429;
I.M. Cheshire, G. Dearnaley and J.M. Poate, Phys. Letters 27A (1968) 304; Proc. Roy. Soc. (London) A311 (1969) 47;
F.F. Komarov and M.A. Khumakov, Phys. Status Solidi (b) 58 (1973) 389.
[52] G.A. Harrower, Phys. Rev. 102 (1956) 340.
[53] M.J. Lynch and J.B. Swan, Australian J. Phys. 21 (1968) 811.
[54] J.F. Hennequin, J. Physique 29 (1968) 1053;
J.F. Hennequin and P. Viaris de Lesegno, Surface Sci. 42 (1974) 50.
[55] C. Benazeth, N. Benazeth and L. Viel, Surface Sci. 65 (1977) 165; Surface Sci. 78 (1978) 625.
[56] A. Russek, Phys. Rev. 132 (1963) 246.
[57] J.D. Garcia, R.J. Fortner and T.M. Kavanagh, Rev. Mod. Phys. 45 (1973) 111.
[58] H.G. Lye and A.J. Dekker, Phys. Rev. 107 (1957) 977.